



Patterns of Transposable Element Distribution around Chromatin Ligation Points Revealed by Micro-C Data Analysis



Alexandr V. Vikhorev¹, Michael M. Rempel¹, Oksana O. Polesskaya¹, Ivan V. Savelev¹, Alexandre A. Vetcher^{2,3,*}  and Max V. Myakishev-Rempel^{1,*} 

¹DNA Resonance Research Foundation, San Diego, CA, USA

² Head of the Nanotechnology lab, Institute of Pharmacy and Biotechnology (IPhB) of RUDN University n.a. P. Lumumba (RUDN), 6 Miklukho-Maklaya Str, Moscow-117198, Russian Federation, Russia

³ Senior Research Scientist, Institute for Bionic Technologies and Engineering, I.M. Sechenov First Moscow State Medical University, 2-4 Bolshaya Pirogovskaya Str-119991 Moscow, Russia

© 2025 The Author(s). Published by Bentham Open.

This is an open access article distributed under the terms of the Creative Commons Attribution 4.0 International Public License (CC-BY 4.0), a copy of which is available at: <https://creativecommons.org/licenses/by/4.0/legalcode>. This license permits unrestricted use, distribution, and reproduction in any medium, provided the original author and source are credited.



* Address correspondence to this author at the DNA Resonance Research Foundation, San Diego, CA, USA, Head of the Nanotechnology lab, Institute of Pharmacy and Biotechnology (IPhB) of RUDN University n.a. P. Lumumba (RUDN), 6 Miklukho-Maklaya Str, Moscow-117198, Russian Federation, Russia and Senior Research Scientist, Institute for Bionic Technologies and Engineering, I.M. Sechenov First Moscow State Medical University, 2-4 Bolshaya Pirogovskaya Str-119991 Moscow, Russia; E-mails: avetcher@gmail.com and max@dnaresonance.org

Published: April 16, 2025



Cite as: Vikhorev A, Rempel M, Polesskaya O, Savelev I, Vetcher A, Myakishev-Rempel M. Patterns of Transposable Element Distribution around Chromatin Ligation Points Revealed by Micro-C Data Analysis. Open Bioinform J, 2025; 18: e18750362357726-SP. <http://dx.doi.org/10.2174/0118750362357726250410070525>

Send Orders for Reprints to
reprints@benthamscience.net

SUPPLEMENT



Fig S1. _ALU. Distribution pattern of Alu transposable elements around chromatin ligation points. The graph shows the density of Alu elements relative to chromatin contact sites, demonstrating their spatial organization in the genome context.

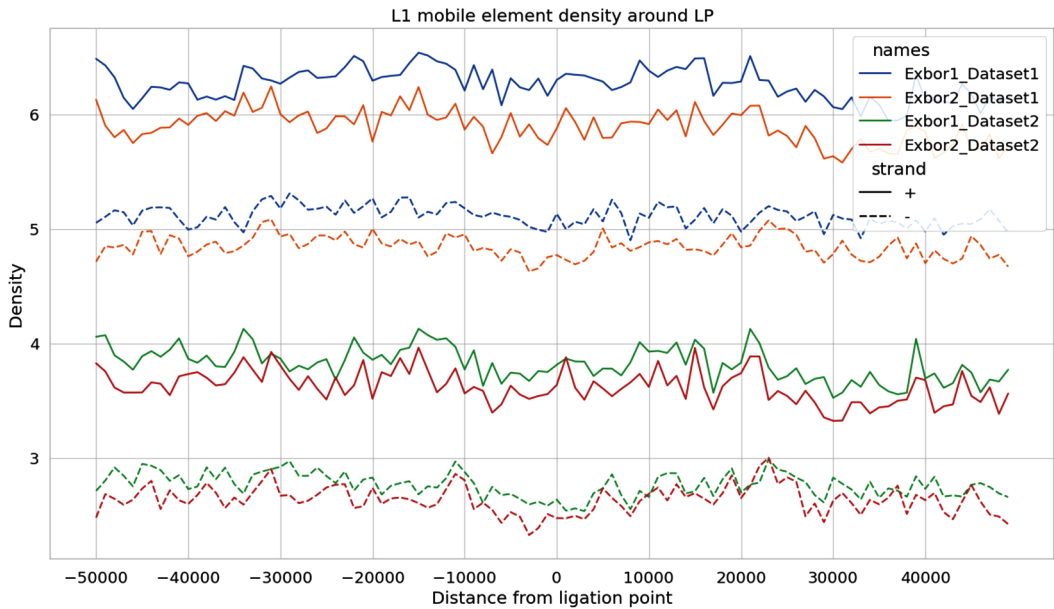


Fig S2. _L1. Density distribution of L1 (LINE-1) transposable elements in relation to chromatin contact points. The plot illustrates the positioning patterns of L1 elements around chromatin ligation sites.



Fig S3. _L2. Analysis of L2 transposable element distribution surrounding chromatin contact points. The figure shows the characteristic arrangement of L2 elements in proximity to chromatin ligation sites.

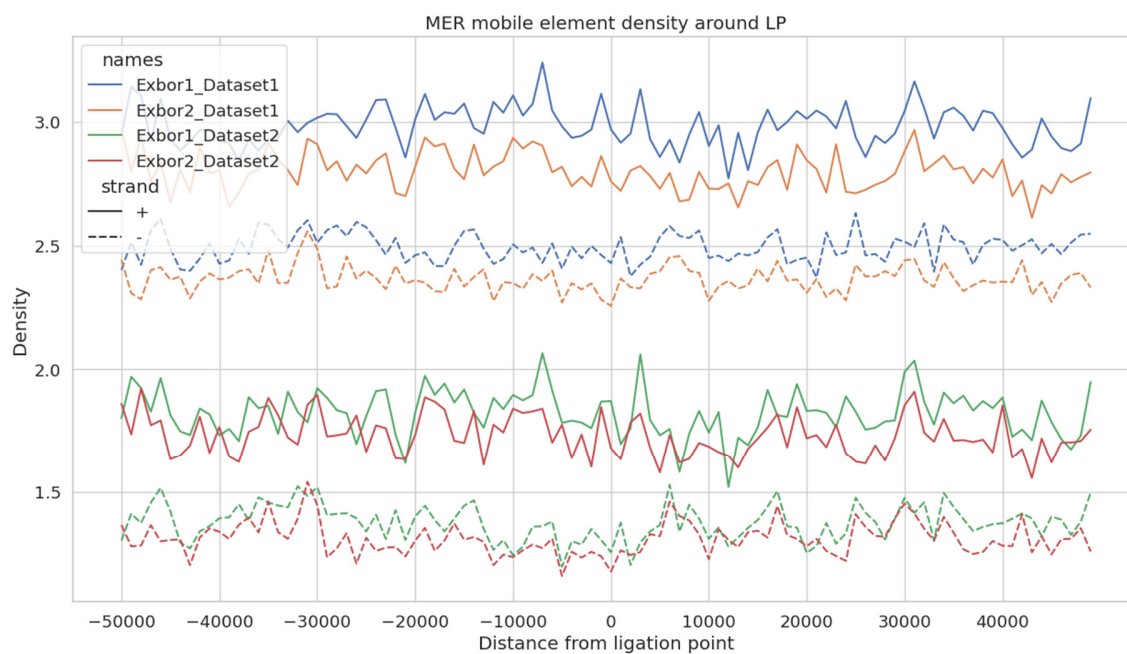


Fig S4. _MER. Spatial distribution of MER transposable elements relative to chromatin contact points, showing their organizational patterns in the genomic landscape.

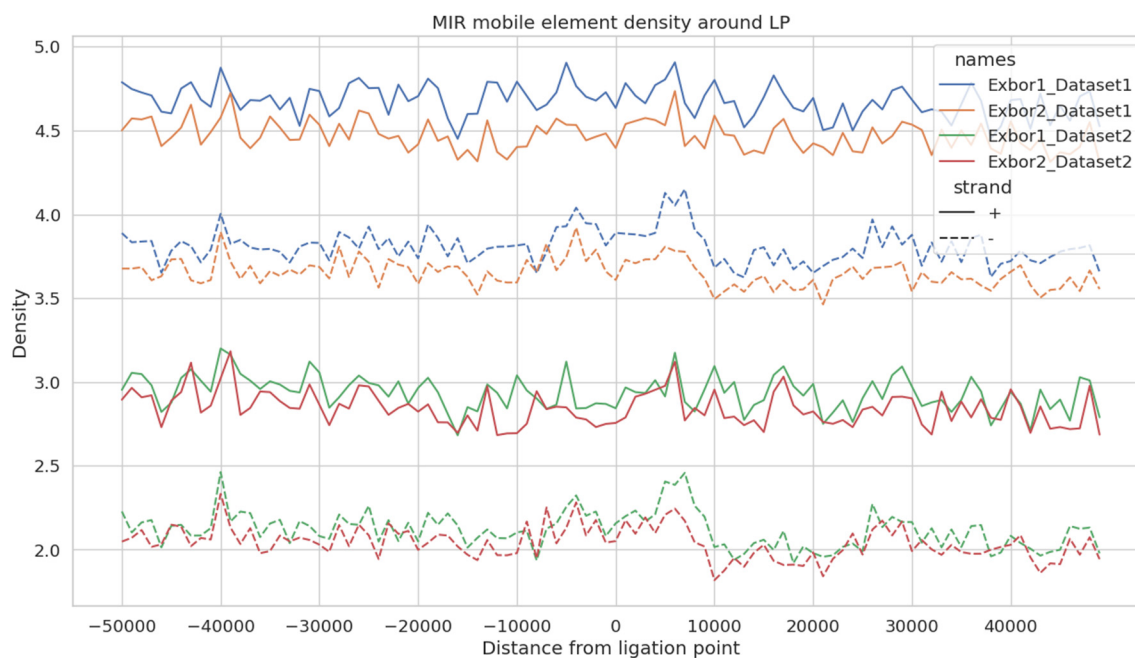


Fig S5. _MIR. Distribution profile of MIR (Mammalian-wide Interspersed Repeat) elements around chromatin ligation points, illustrating their positioning patterns in relation to chromatin contacts.



Fig S6. _MLT. Density plot showing the distribution of MLT transposable elements around chromatin contact points, revealing their spatial arrangement patterns.

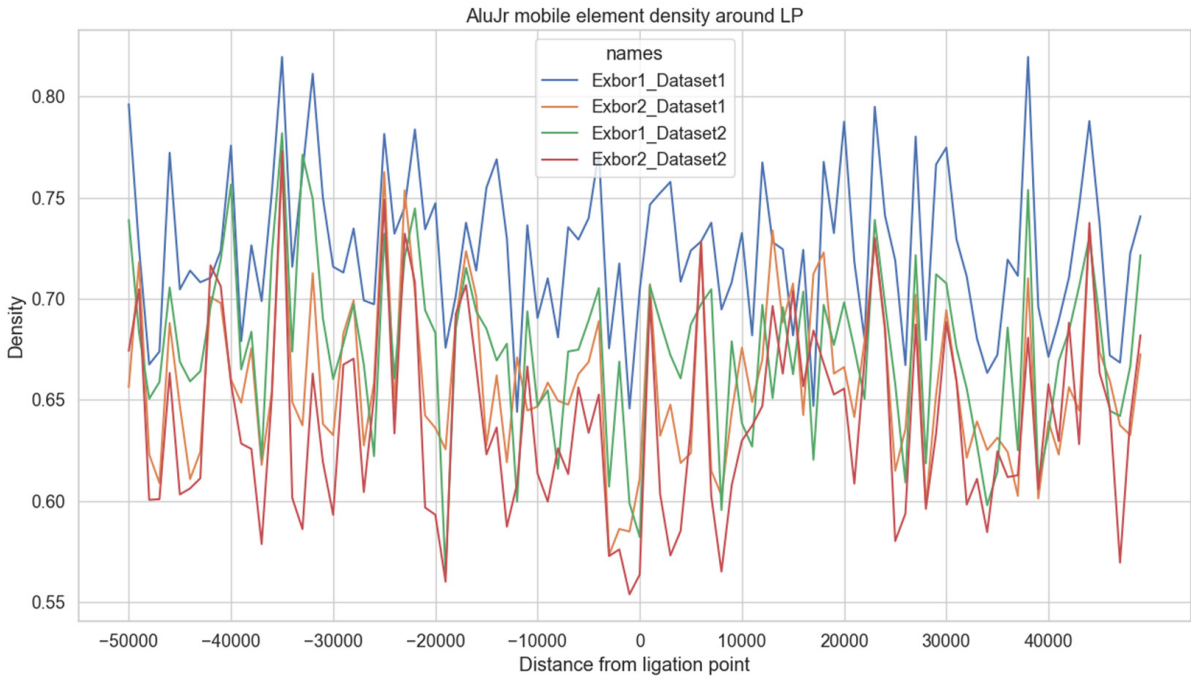


Fig S7. _AluJr. Specific distribution pattern of AluJr subfamily elements around chromatin ligation points, demonstrating their unique spatial organization.

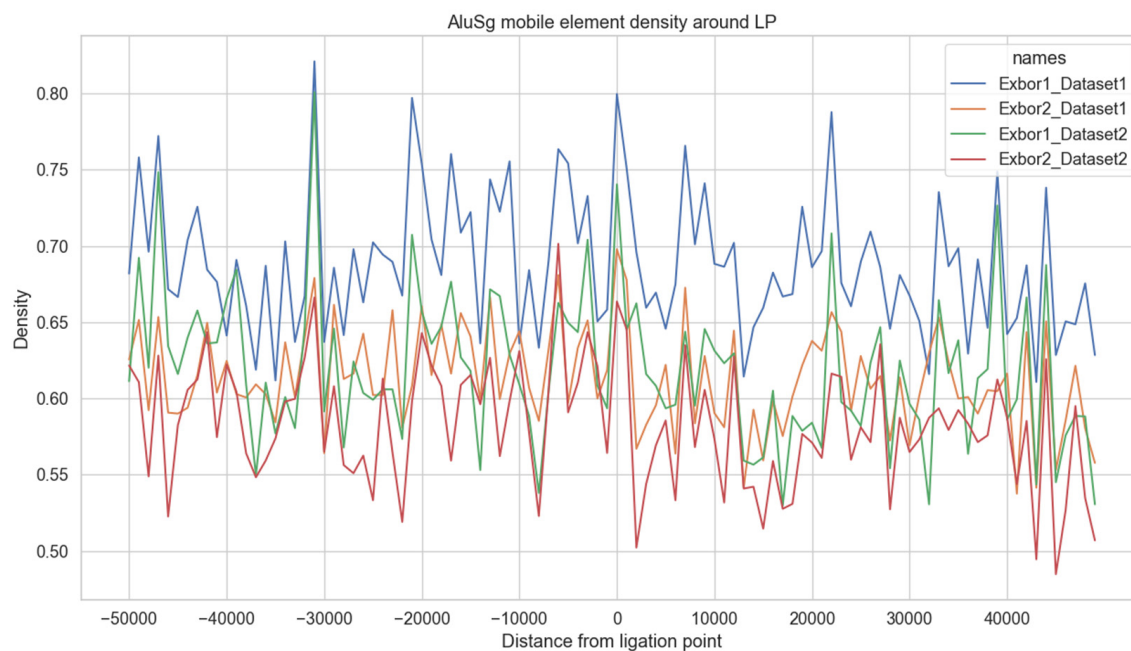


Fig S8. _AluSg. Analysis of AluSg subfamily element distribution in relation to chromatin contact points, showing their characteristic positioning patterns.

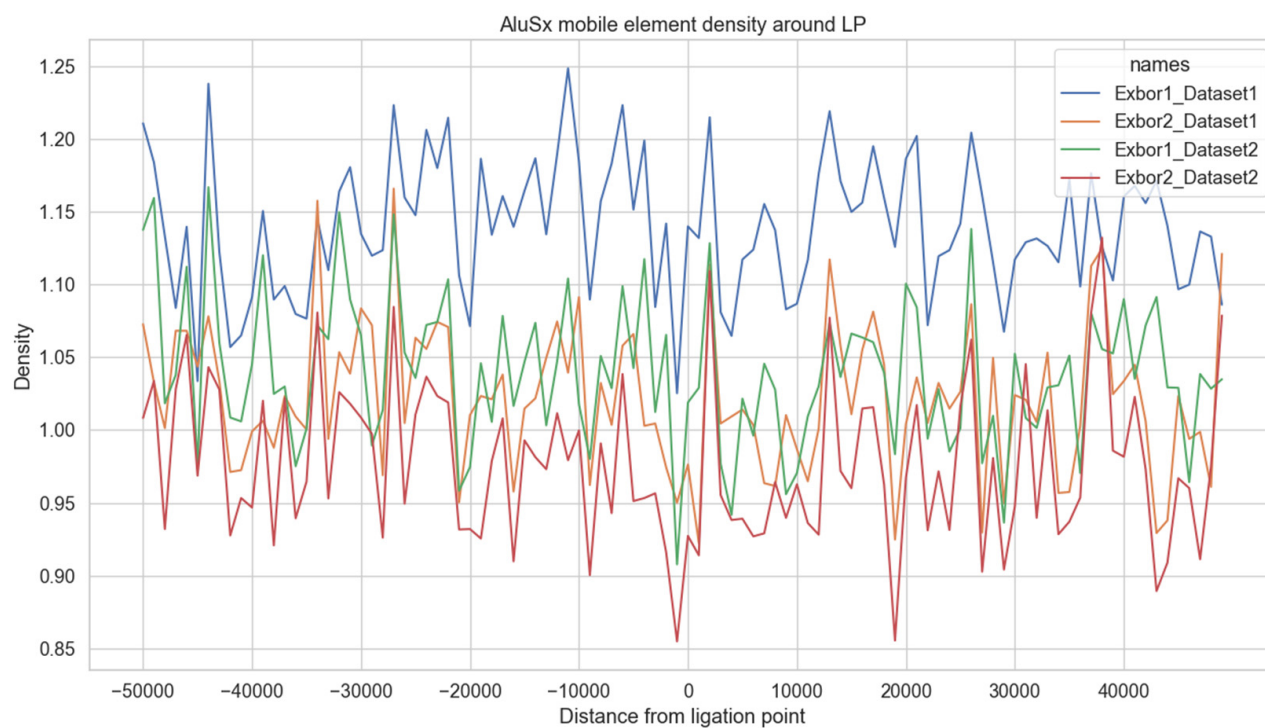


Fig S9. _AluSx. Spatial distribution profile of AluSx subfamily elements around chromatin ligation points, illustrating their specific arrangement patterns.

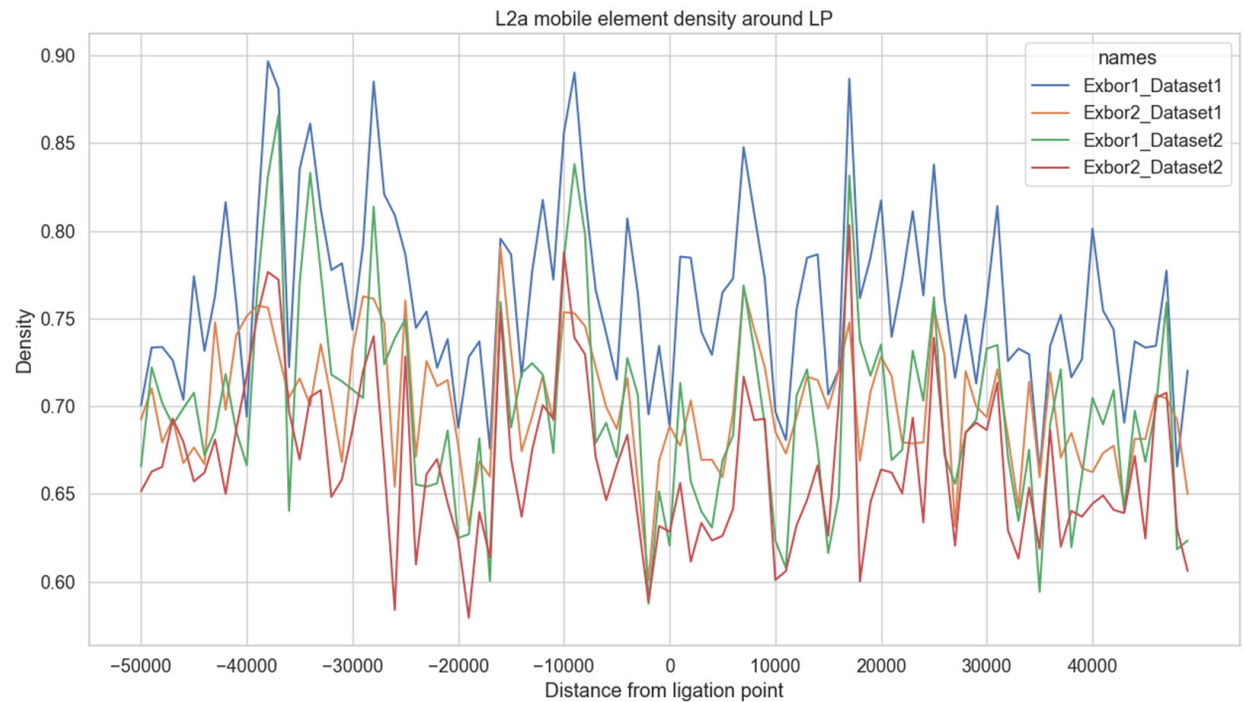


Fig S10. _L2a. Distribution analysis of L2a subfamily elements in proximity to chromatin contact points, showing their distinct positioning patterns.

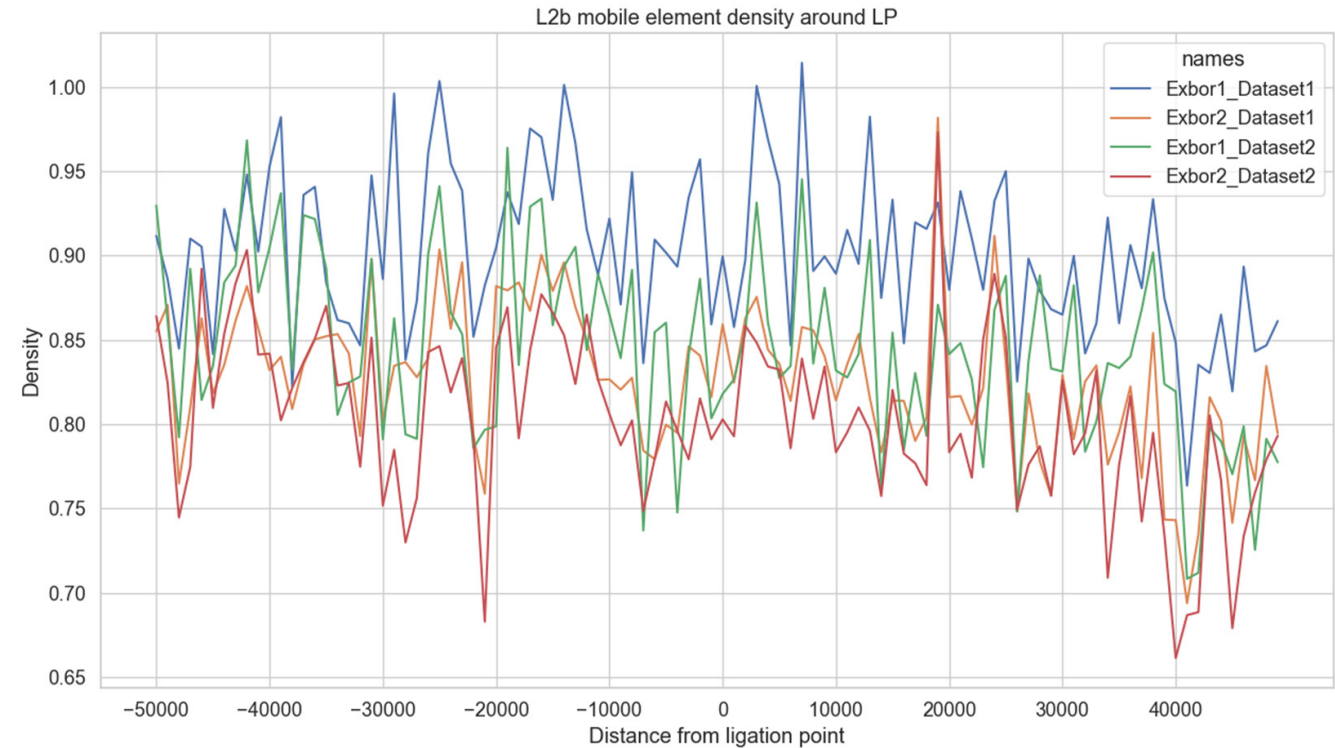


Fig S11. _L2b. Density plot showing the distribution of L2b subfamily elements around chromatin ligation points, revealing their specific spatial organization.

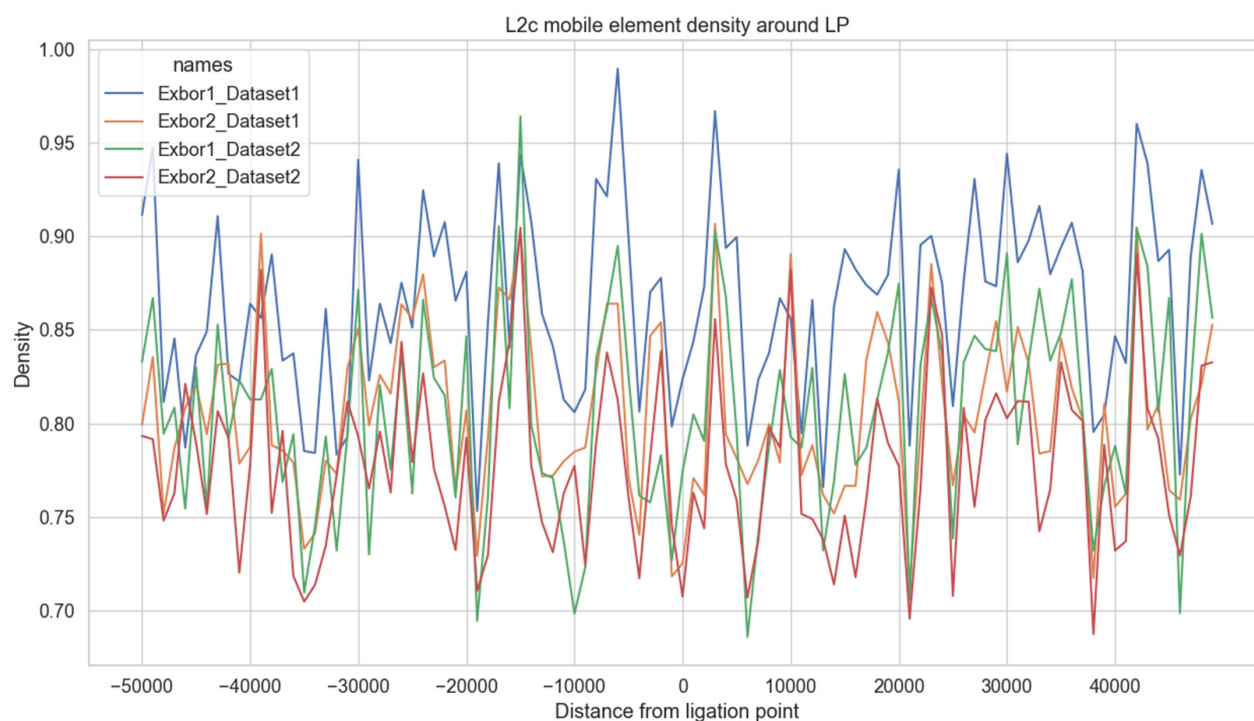


Fig S12. _L2c. Analysis of L2c subfamily element distribution relative to chromatin contact points, demonstrating their characteristic arrangement patterns.

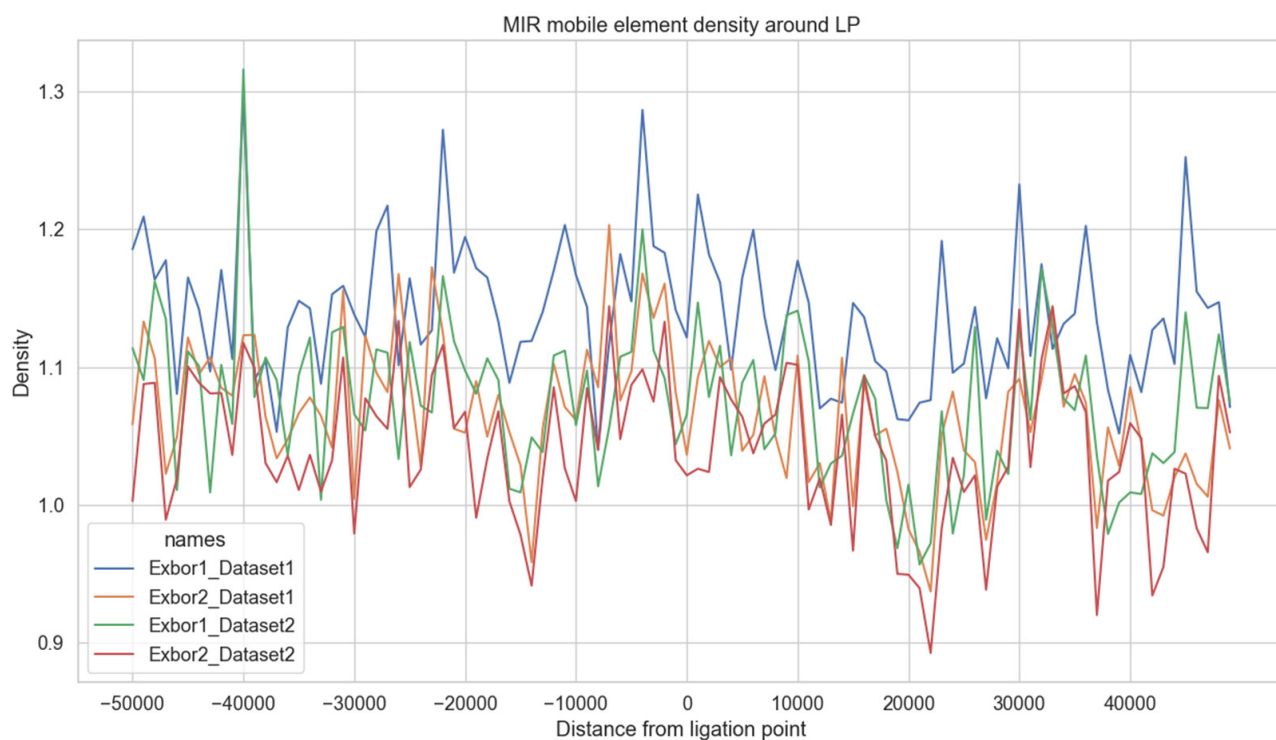


Fig S13. _MIR subfamily. Distribution pattern of MIR subfamily elements around chromatin ligation points, showing their specific spatial organization in the genome.

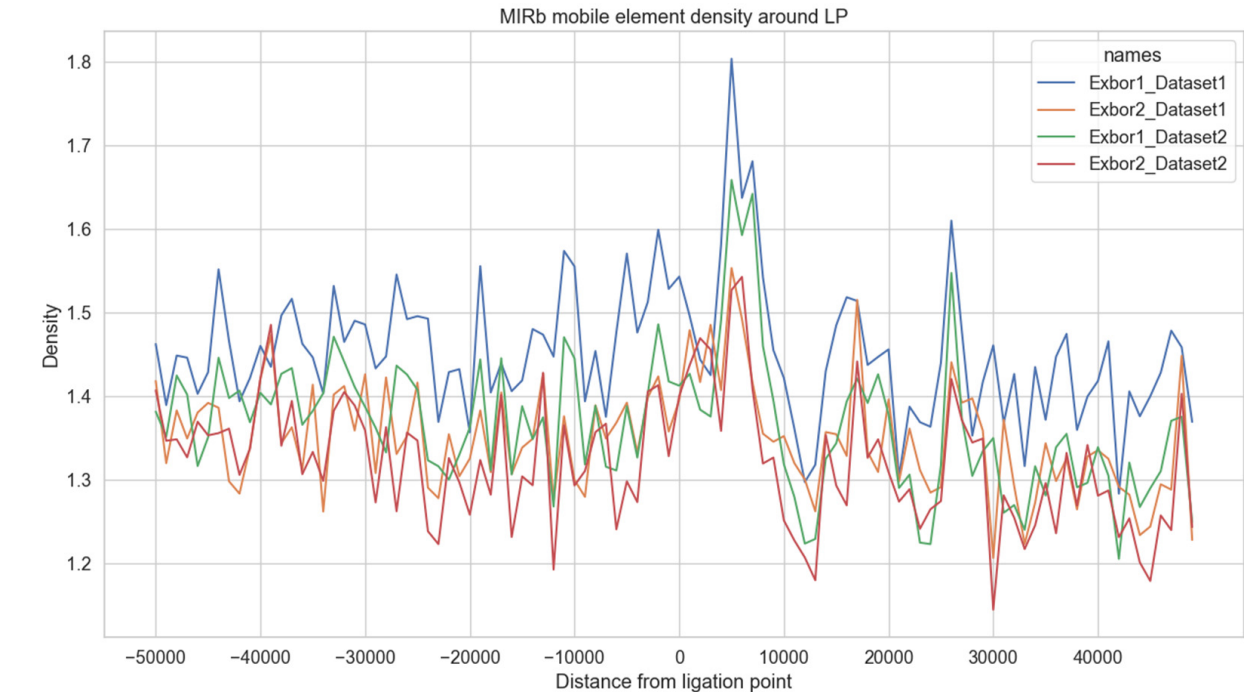


Fig S14. _MIRb. Spatial distribution analysis of MIRb subfamily elements in relation to chromatin contact points, illustrating their positioning patterns.

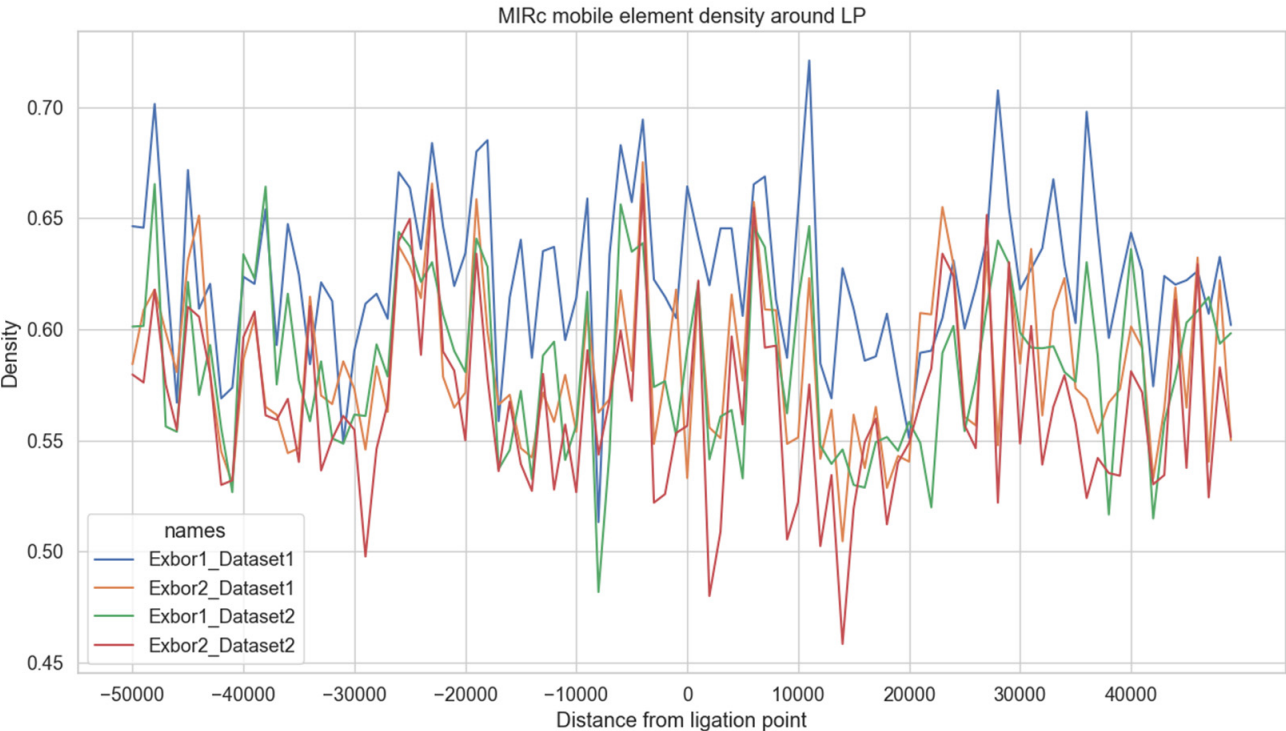


Fig S15. _MIRc. Distribution profile of MIRc subfamily elements around chromatin ligation points, showing their characteristic arrangement patterns.

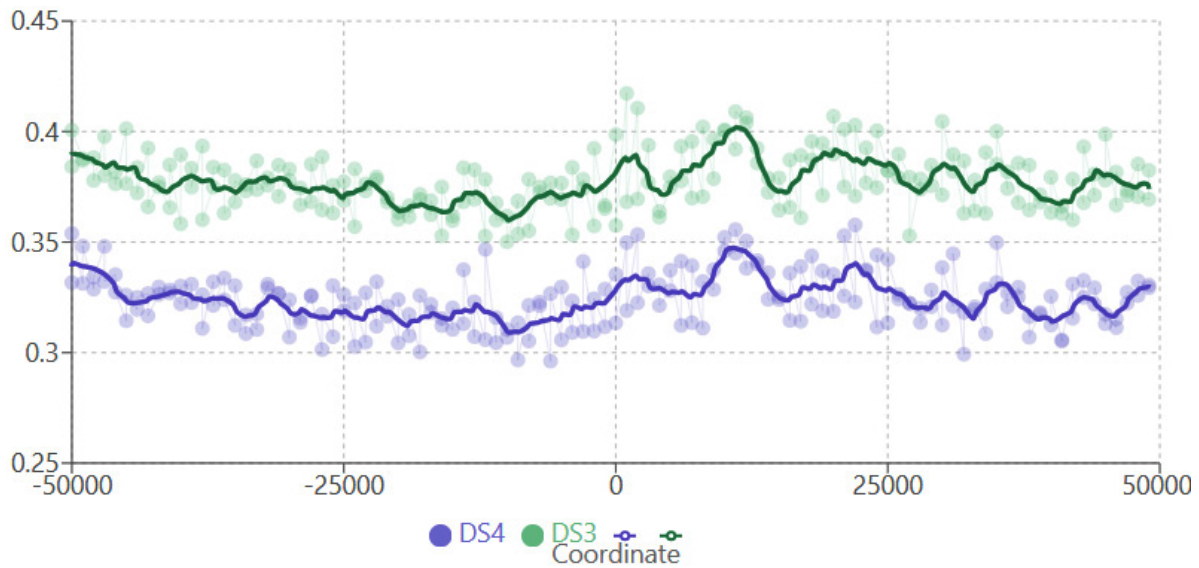


Fig S16. _DS3-DS4 Transposon L2b DS3 is correlated with DS4 (strands averaged, strand info ignored) Correlation analysis of L2b transposon distribution between datasets DS3 and DS4, with strand information combined, demonstrating the reproducibility of positioning patterns.

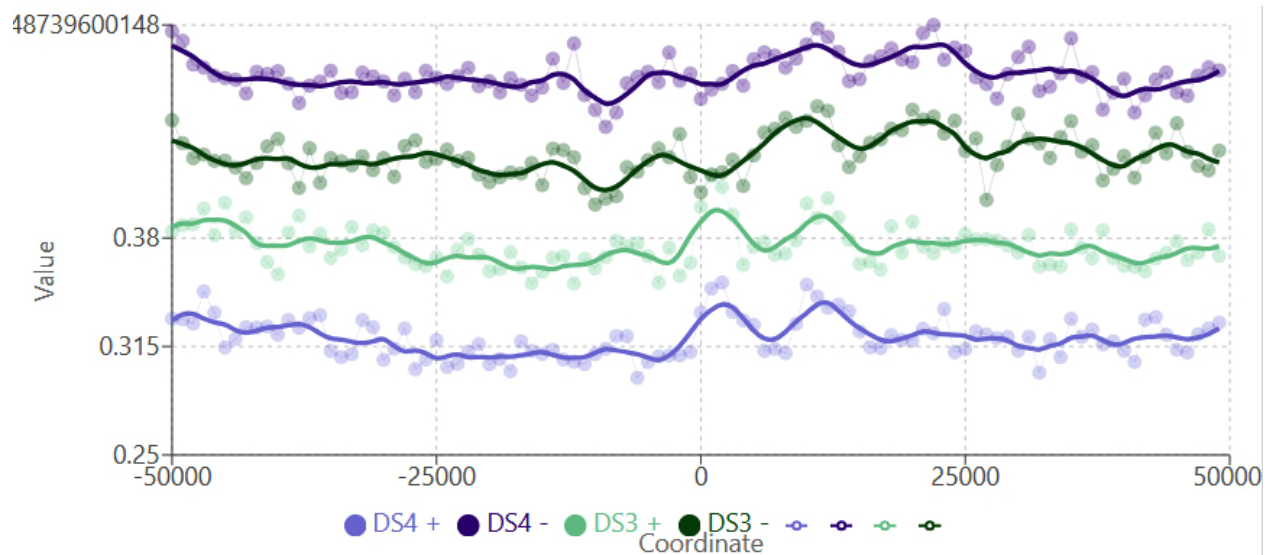


Fig S17. _DS3-DS4 Transposon L2b DS3 is correlated with DS4 (strands plotted separately). Strand-specific correlation analysis of L2b transposon distribution between datasets DS3 and DS4, showing distinct patterns for plus and minus strands.

Correlation

The following graphs are correlations for density curves between Datasets D1, D2, D3, D4. The transposon subfamily is marked on the top of each graph.

Correlation Analysis of Transposable Element Distributions These correlation plots demonstrate the reproducibility of transposable element density patterns around chromatin contact points across different datasets and methods. Each plot shows pairwise correlations between biological replicates, with lighter colors

indicating stronger correlations. Plus (+) and minus (-) strands are analyzed separately to reveal strand-specific patterns. Correlation values between corresponding strands of biological replicates typically reach 0.7-0.8, while correlations between opposite strands remain below 0.2, quantitatively confirming strand specificity. Results are shown for Alu (X), L1 (Y), L2a-c (Z) and their subfamilies. The consistent patterns across Hi-C (DS3, DS4) and Micro-C (DS1, DS2) datasets validate the biological authenticity of these organizational features.

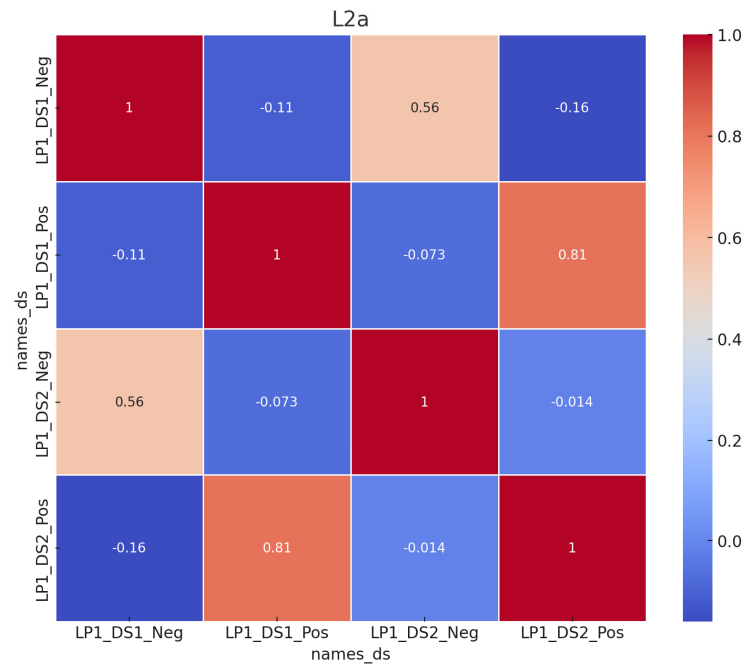


Fig S18. Correlation Analysis, Transposon L2. Series of correlation plots showing pairwise comparisons between datasets D1, D2, D3, and D4 for various transposable element subfamilies. The plots demonstrate the reproducibility of density patterns across different experimental methods and biological replicates. Correlation values between corresponding strands typically range from 0.7-0.8, while opposite strand correlations remain below 0.2, confirming strand specificity.

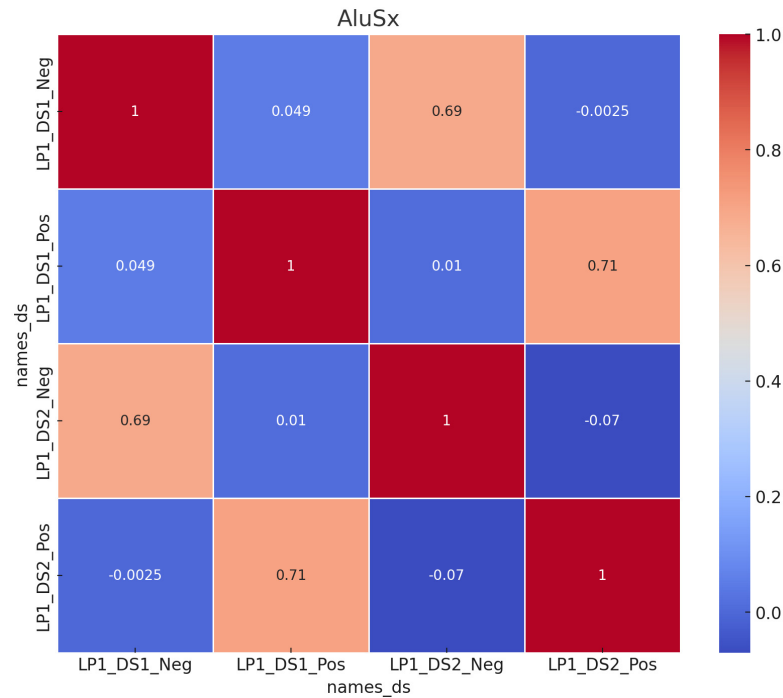


Fig S19. Correlation Analysis AluSx. Series of correlation plots showing pairwise comparisons between datasets D1, D2, D3, and D4 for various transposable element subfamilies. The plots demonstrate the reproducibility of density patterns across different experimental methods and biological replicates. Correlation values between corresponding strands typically range from 0.7-0.8, while opposite strand correlations remain below 0.2, confirming strand specificity.

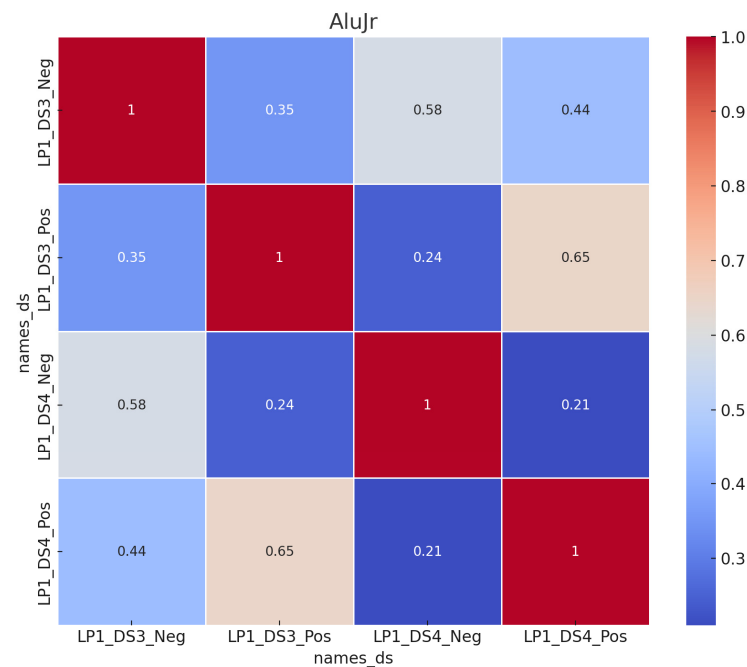


Fig S20. Correlation Analysis AluJr. Series of correlation plots showing pairwise comparisons between datasets D1, D2, D3, and D4 for various transposable element subfamilies. The plots demonstrate the reproducibility of density patterns across different experimental methods and biological replicates. Correlation values between corresponding strands typically range from 0.7-0.8, while opposite strand correlations remain below 0.2, confirming strand specificity.

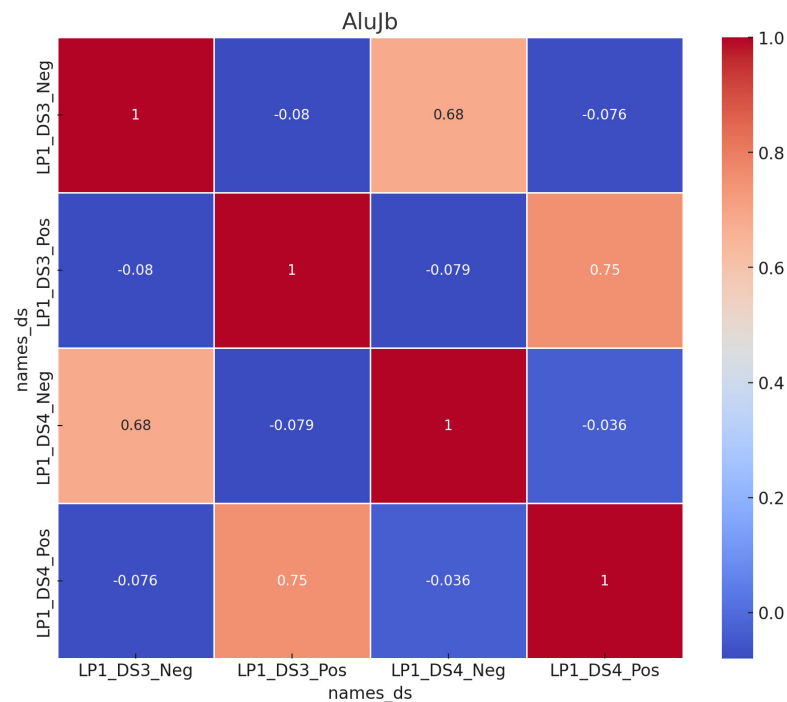


Fig S21. Correlation Analysis AluJb. Series of correlation plots showing pairwise comparisons between datasets D1, D2, D3, and D4 for various transposable element subfamilies. The plots demonstrate the reproducibility of density patterns across different experimental methods and biological replicates. Correlation values between corresponding strands typically range from 0.7-0.8, while opposite strand correlations remain below 0.2, confirming strand specificity.

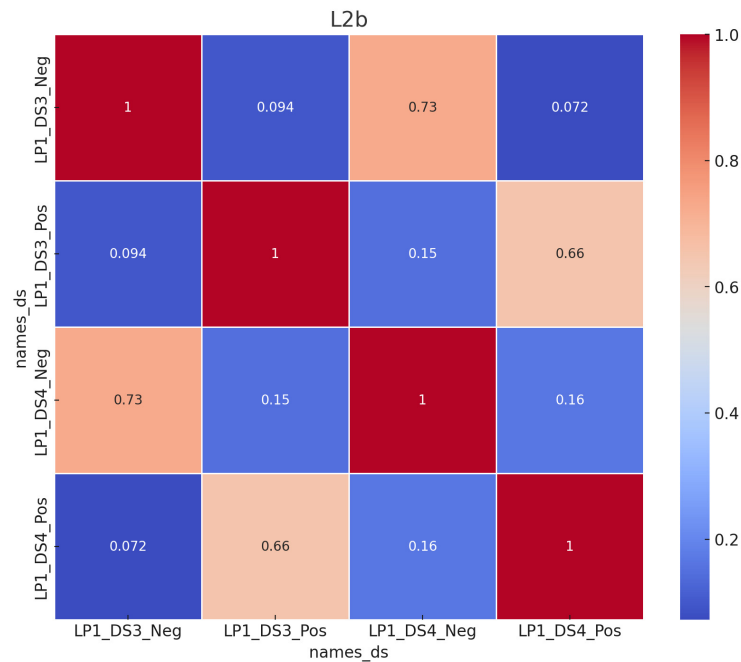


Fig S22. Correlation Analysis L2b. Series of correlation plots showing pairwise comparisons between datasets D1, D2, D3, and D4 for various transposable element subfamilies. The plots demonstrate the reproducibility of density patterns across different experimental methods and biological replicates. Correlation values between corresponding strands typically range from 0.7-0.8, while opposite strand correlations remain below 0.2, confirming strand specificity.

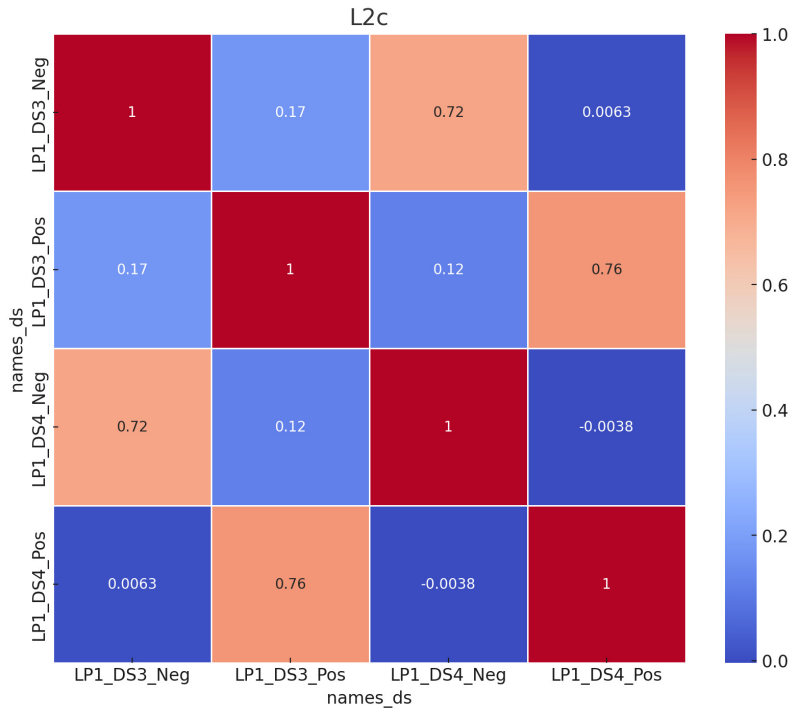


Fig S23. Correlation Analysis L2C. Series of correlation plots showing pairwise comparisons between datasets D1, D2, D3, and D4 for various transposable element subfamilies. The plots demonstrate the reproducibility of density patterns across different experimental methods and biological replicates. Correlation values between corresponding strands typically range from 0.7-0.8, while opposite strand correlations remain below 0.2, confirming strand specificity.

Random Controls

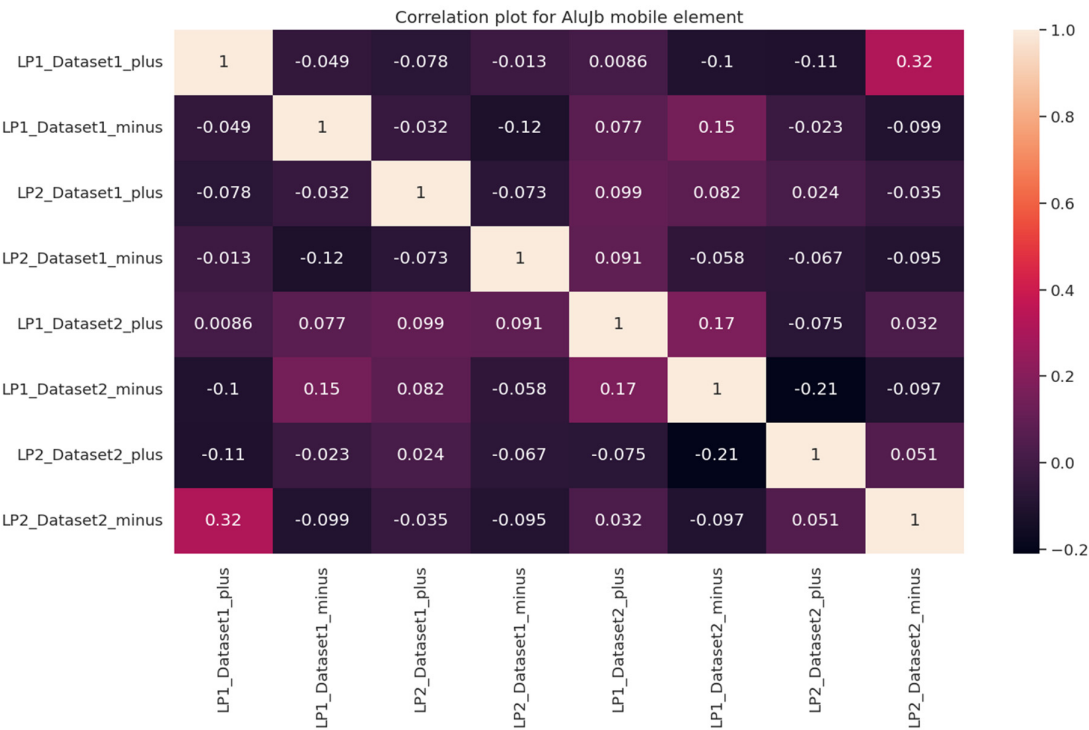


Fig S24. Random controls, AluJb Analysis of transposable element distribution patterns using randomized control datasets, validating the specificity of the observed patterns in the experimental data.